# Critical Branching Captures Activity in Living Neural Networks and Maximizes the Number of Metastable States

Clayton Haldeman and John M. Beggs*

*Department of Physics, Indiana University, Bloomington, Indiana, USA*
(Received 15 September 2004; published 7 February 2005)

Recent experimental work has shown that activity in living neural networks can propagate as a critical branching process that revisits many metastable states. Neural network theory suggests that attracting states could store information, but little is known about how a branching process could form such states. Here we use a branching process to model actual data and to explore metastable states in the network. When we tune the branching parameter to the critical point, we find that metastable states are most numerous and that network dynamics are not attracting, but neutral.

The brain, though tremendously complex, consists of many apparently similar neurons. This homogeneity has led researchers to borrow concepts from physics in an effort to explain how collective phenomena could emerge from interactions. For example, several models predict that neural networks should operate optimally near a critical point like that in a continuous phase transition [1–4], and exhibit numerous metastable states like those seen in a spin glass [5,6]. The critical point may allow optimum information transmission within a network [7], while metastable states may be useful for information storage [5,6].

Recent experiments support these predictions. Cultured brain slices of rat cortex can be kept alive for several weeks while microelectrode arrays monitor their activity. These networks are typically quiescent for several seconds, and then experience a spontaneous burst of local field potential activity that drives the voltage levels at some electrodes above a threshold. Within 20 ms, the activity at these electrodes may spread to other electrodes before the network returns to quiescence and starts another burst. The total number of electrodes activated gives the size of the burst. Interestingly, the distribution of burst sizes recorded over 10 h follows a power law [7], similar to the distribution of cluster sizes seen at the critical point in a continuous phase transition [8] or the number of toppled sites in critical avalanche models [9]. In addition, activity on one electrode is on average followed by activity on one other electrode in the next time step. This can be expressed by the branching parameter, $\sigma$, which is observed experimentally as the ratio of the number of descendant electrodes to the number of ancestor electrodes[10]

$$\sigma = \frac{n_{\text{descendants}}}{n_{\text{ancestors}}}. \qquad (1)$$

Subcritical processes ($\sigma < 1$) produce activity that dies out, critical processes ($\sigma = 1$) produce activity that is nearly sustained, and supercritical processes ($\sigma > 1$) produce growing activity. The branching parameter $\sigma$ is very close to the critical value of one for cortical cultures [7], indicating that activity can spread as a critical branching process [10]. While branching processes are often stochastic [9,10], activity in these cortical cultures does not propagate in a random manner but in preferred paths that are repeated significantly more than chance over several hours [11,12]. Actual and shuffled data are compared to estimate chance occurrence of repeating activity patterns [11,12]. Significantly repeating activity also occurs in noncultured acute cortical slices [13]. These activation patterns resemble the metastable states a broad class of attractor neural network models generates [5,6], further supporting the predictions of neural network theory.

These new results from cortical tissue raise several questions: How do the branching parameter $\sigma$ and the number of metastable states relate? If such states are useful for storing information, we expect that brain networks would operate in a regime where these states are most numerous. Also, how does the branching parameter influence network dynamics? While many neural network models predict that metastable states should have attracting dynamics [5,6], these dynamics have not been examined in a branching network.

*Methods.*—To address these issues, we measured network performance as we swept $\sigma$ from subcritical to supercritical values. Because manipulating $\sigma$ precisely in experiments with cortical tissue is difficult, we chose to pursue these questions using a branching network model. This model represents each recording electrode by a binary processing unit that can be either on (1) or off (0), since an electrode can receive either suprathreshold or subthreshold input. The model consists of a sheet of $N \times N$ processing units with each unit randomly connected to $C$ other units, giving the network a recurrent, rather than a feed-forward [7], architecture. Each connection from unit $i$ to unit $j$ has a probability $p_{ij}$ of transmitting that is randomly chosen and then fixed. In this context, the branching parameter of unit $i$ is given by the sum of probabilities

emanating from that unit:

$$\sigma_i = \sum_{j=1}^{C} p_{ij}, \qquad (2)$$

where $0 \le p_{ij} \le 1$ and $0 \le \sigma_i \le C$. $\sigma_i$ is equivalent to the expected number of descendants an active unit $i$ produces [10]. Transmission probabilities for each unit are not generally the same, but we constrain the sum of these probabilities so that $\sigma_i = \sigma$ for all $i$ to set the branching parameter for the entire network ($\sigma$). Unit $j$ at time step $t + 1$ becomes active only if unit $i$ in the previous time step $t$ is active and the connection between them transmits. A connection transmits if rand $\le p_{ij}$, where rand is a uniformly distributed random number drawn from the interval [0, 1]. Processing units update at each time step to simulate the propagation of activity through the network. Even though the network is nondeterministic, certain preferred patterns of activity can develop as a result of the fixed underlying transmission probabilities. A network can operate in "spontaneous" mode where each unit has a small probability of being spontaneously active ($p_{spont} = 0.001$) [7]. We use this mode to examine how the branching parameter influences the burst size distribution. Alternatively, a network can operate in "driven" mode where a subset $n$ of the $N^2$ units ($n < N^2$) receives a random binary input configuration at the same time step. The choice of $N$, $C$, and $\sigma$ determines network type. This model does not account for detailed neural circuitry underlying the local field potentials recorded at the electrodes, which has been explored elsewhere [14]. Rather, it seeks to capture only those features of the network that are accessible from the microelectrode data. This intentionally parsimonious approach reveals general features that might lead to a universal class of network behaviors. As we will show, some model details do not affect the results.

We define a metastable state as a set of network output configurations that are more similar to each other than we would expect by chance. We extract such states with procedures similar to those previously used to identify significantly repeating activity patterns in data from living neural networks [11,12]. Briefly, a network operates in driven mode with $n$ randomly chosen input units. The activity of the network evolves over $T$ time steps and we record the status of $n$ output units, randomly chosen but excluding input units, as the binary output configuration. We repeat this process $m$ times. Similarity between output configurations $\Omega^i = (\omega_1^i, \omega_2^i, \omega_3^i, \ldots \omega_n^i)$ and $\Omega^j = (\omega_1^j, \omega_2^j, \omega_3^j, \ldots \omega_n^j)$ can range from 0 to 1, defined as their intersection divided by their union, as in [15]:

$$\mathrm{Sim}(\Omega^i, \Omega^j) = \frac{\langle \Omega^i, \Omega^j \rangle}{\langle \Omega^i, \Omega^i \rangle + \langle \Omega^j, \Omega^j \rangle - \langle \Omega^i, \Omega^j \rangle}, \qquad (3)$$

where $\langle \cdot, \cdot \rangle$ indicates a dot product. We then clustered the $m$ output configurations using a greedy algorithm and com-

pared them to 20 sets of $m$ clustered configurations obtained from shuffled network output. To assess the probability of chance agreement, we shuffled the network output using event-count matched shuffling, a method that produces the fewest false positives for neural data [11,16]. We declared any cluster of output configurations with a higher average similarity value than all clusters produced by 20 shuffled data sets significant at the $p < 0.05$ level and considered it a metastable state. The similarities of all output configurations with each other are visualized in a similarity matrix $M_{sim}$, where each element is given by: $M_{sim}(i, j) = \mathrm{Sim}(\Omega^i, \Omega^j)$.

To quantify network dynamics, we measure the rate of divergence of trajectories in phase space by estimating a Boolean version of the Lyapunov exponent $\lambda$ similar to that used by Derrida [17,18]. We apply a random input configuration to the network and follow the network's response over $T$ time steps. While following this trajectory, we repeatedly apply a small random input perturbation that differs from the current network configuration by a Pythagorean distance $d_{in}$. We then measure the resulting distance between trajectories, $d_{out}$, a few time steps after the perturbation. The Boolean Lyapunov exponent in bits/time is then:

$$\lambda = \frac{1}{T} \sum_{1}^{n} \log_2\left(\frac{d_{out}}{d_{in}}\right), \qquad (4)$$

where $n$ is the number of perturbations[18,19].

*Results.*—We tested whether this parsimonious model generated burst size distributions and metastable states similar to those seen in living networks. Because the data showed critical branching and were recorded with a 60-channel microelectrode array, we used $\sigma = 1$ and $N^2 = 64$ to simulate experimental results. We also used $C = 64$, because in the data activity in a given electrode sometimes preceded activity in every other electrode, indicating possible functional connections between all units. Figure 1(a) shows a model with these parameters produces a power law distribution of burst sizes with a slope near $-3/2$ as in experimental neural networks [7]. In addition, the model
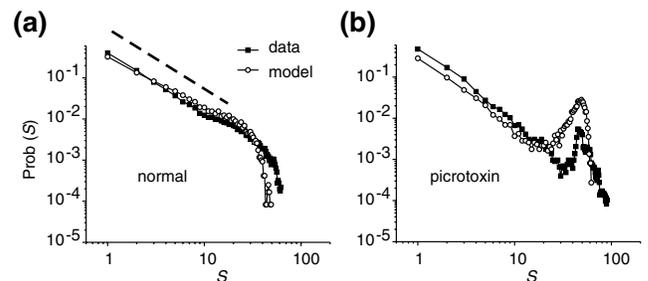


FIG. 1. Power law distribution of burst sizes from cultures. (a) Normal cultures correspond to $\sigma = 1$ in the model. Dashed line gives slope $= -3/2$. (b) Cultures made supercritical by picrotoxin (2 $\mu$M) display a peak near $S = 60$. The model reproduces experimental data from [7].

mimicked the doubly peaked distribution produced when we bathed the cortical cultures in picrotoxin, an agent that selectively blocked inhibition and increased $\sigma$ [Fig. 1(b)] [7]. The hump in the distribution near $S = 60$ is caused by activity that propagates over the entire electrode array before dying out. The model also produced similarity matrices and metastable states similar to those in living networks (Fig. 2), suggesting that the simple branching network qualitatively captured salient features of cortical slice culture.

Using this model, we determine the branching parameter's influence on the number of metastable states. We ran simulations in driven mode increasing $\sigma$ from 0.00 to 3.00 in increments of 0.02. For small networks ($N^2 \leq 64$) the number of metastable states peaked at clearly supercritical values of $\sigma$ [$\sigma \geq 1.6$; Fig. 3(a)], but for larger networks this peak gradually approached the critical value of $\sigma = 1.0$ [for $N^2 = 2500$, $\sigma = 1.00$; best least-squares fit single exponential for all data: $\sigma = 1.03 \pm 0.01$, mean $\pm$ s.d., $R^2 = 0.98$; Fig. 3(b)]. While most of these simulations used few connections to reduce computation times ($C = 4$), increasing $C$ to 16 or 32 did not change appreciably our results [Fig. 3(b)].

The similarity matrices the three types of networks produced offer an intuitive explanation of these results. Subcritical networks have units weakly coupled so their activity is uncorrelated, producing few output configurations that share more than chance similarities [Fig. 2(b), left]. In contrast, supercritical networks have units connected so strongly that activation of any unit usually activates the whole network. The one resulting metastable state was highly ordered, but inhibited other states [Fig. 2(b), right]. When the branching parameter was critical ($\sigma = 1.0$), a mixture of variety and order prevailed,

allowing several different clusters of output configurations to achieve significance [Fig. 2(b), center], thus maximizing the number of metastable states.

We also investigated dynamics in the branching networks. For all networks, the Boolean Lyapunov exponent $\lambda$ did not settle at one value, but wandered itinerantly near a mean (Fig. 4) [20]. In critical networks, this mean was indistinguishable from zero ($\sigma = 1$, $\lambda \cong 0$), producing neutral dynamics on average. By neutral, we mean that the distance between nearby trajectories remained nearly constant over time. Supercritical networks had chaotic dynamics ($\sigma > 1$, $\lambda \geq 0$), where small initial distances between trajectories were amplified over time. Subcritical networks had attracting dynamics ($\sigma < 1$, $\lambda \leq 0$), where distances between trajectories shrank over time. Thus the branching parameter determined three dynamical regimes.

Bursting in cortical slice cultures differs from the more continuous activity seen in awake, behaving animals [21]. However, others have shown that when $\sim$0.6 cm$^2$ slabs of cortical tissue *in vivo* are isolated by cutting from incoming connections, they burst in ways remarkably similar to cortical cultures [22]. When slabs are made larger, bursting becomes more frequent, suggesting that slabs the size of the entire cortical mantle would produce continuous
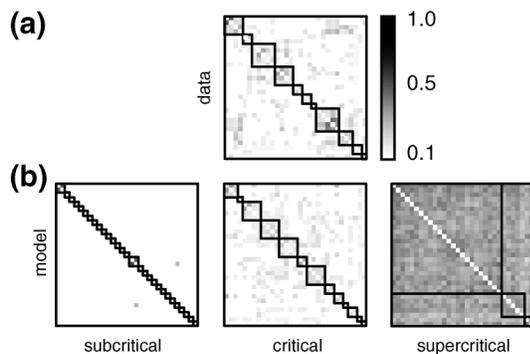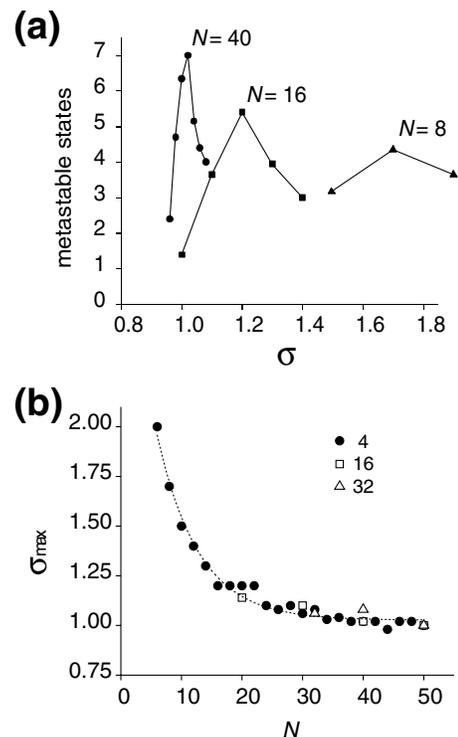
FIG. 2. Model reproduces metastable states in culture. (a) Similarity matrix from cortical cultures. Darker pixels along the diagonal indicate similar output configurations, while boxes selected by the clustering algorithm indicate possible metastable states. (b) Similarity matrices from the model. The critical matrix resembles experimental data, with most boxes high-contrast. The contrast of a box typically predicts its statistical significance, which we determine by comparison to shuffled data [11,12]. Experimental data from [7].

FIG. 3. The number of metastable states is maximal at the critical point. (a) Number of metastable states plotted against $\sigma$. Peaks become sharper and closer to $\sigma = 1.0$ for larger networks. (b) The number of metastable states is maximal at $\sigma = 1.0$ for largest network, regardless of the number of connections per unit (4, 16, 32). Fit for all data asymptotically approaches $\sigma = 1.03 \pm 0.01$.
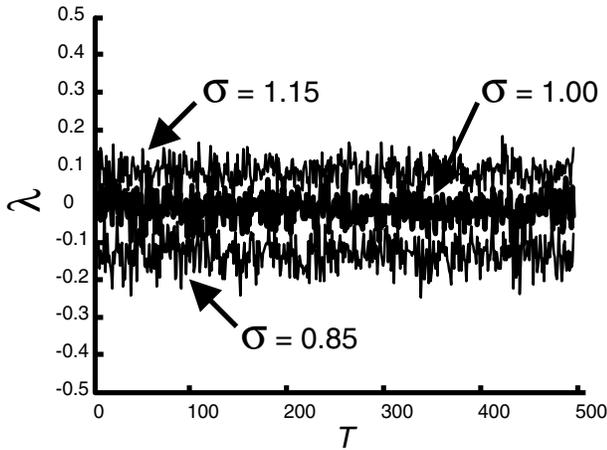
FIG. 4. At the critical point, dynamics hover itinerantly near neutral. Local time estimate of the Boolean Lyapunov exponent, $\lambda$ over 500 time steps for different values of $\sigma$. For upper, middle, and lower traces $\lambda = 0.0887 \pm 0.0329$, $0.0086 \pm 0.0364$, $-0.1282 \pm 0.0423$, respectively. The network has $N = 80$, $C = 40$.

background activity [22]. Such work strongly implies that local cortical networks in isolation intrinsically burst. Nevertheless, because *in vitro* and *in vivo* activity patterns are different, caution should be exercised when extrapolating the results of this model to information processing in the awake, behaving brain.

In conclusion, our parsimonious branching network model captures both the critical power law distribution of burst sizes and the metastable states seen in cortical culture. This model shows that the number of metastable states is maximal when the branching parameter is critical, perhaps for the same reason that cluster size diversity is maximized at critical probability in percolation models [23]. While the dynamics of metastable states in living neural networks are still unknown, that network dynamics at the critical point are neutral rather than strongly attracting contrasts with previous neural models which used attracting dynamics to implement content-addressable memory [5,6]. Although neutral dynamics cannot easily support content addressability, they can support rapid, parallel computations with invariant output [24] and allow maximal control without sacrificing stability. Metastable states which store information [11] need not have attracting dynamics.

Previous work using a feed-forward branching network model also showed that information transmission is maximal at the critical point [7], corresponding to the well-known result that the correlation length diverges at the critical point during a continuous phase transition [8] and is consistent with $\lambda \cong 0$, which we interpret to mean that there is minimal information loss about the initial conditions of a trajectory[25]. Together, our findings suggest that small cortical networks operate near the critical point to simultaneously optimize information storage and transmission, two functions that are crucial for neural computation [26].

*Corresponding author: jmbeggs@indiana.edu

[1] C. W. Eurich, J. M. Herrmann, and U. A. Ernst, Phys. Rev. E **66**, 066137 (2002).
[2] A. V. Herz and J. J. Hopfield, Phys. Rev. Lett. **75**, 1222 (1995).
[3] P. Bak and D. R. Chialvo, Phys. Rev. E **63**, 031912 (2001).
[4] S. Bornholdt and T. Rohl, Phys. Rev. E **67**, 066118 (2003).
[5] J. J. Hopfield, Proc. Natl. Acad. Sci. U.S.A. **79**, 2554 (1982).
[6] D. J. Amit, *Modeling Brain Function: The World of Attractor Neural Networks* (Cambridge University Press, Cambridge, England, 1989).
[7] J. M. Beggs and D. Plenz, J. Neurosci. **23**, 11167 (2003).
[8] H. E. Stanley, *Introduction to Phase Transitions and Critical Phenomena* (Clarendon Press, Oxford, 1971).
[9] M. Paczuski, S. Maslov, and P. Bak, Phys. Rev. E **53**, 414 (1996).
[10] T. E. Harris, *The Theory of Branching Processes* (Dover Publications, New York, 1989).
[11] J. M. Beggs and D. Plenz, J. Neurosci. **24**, 5216 (2004).
[12] R. Segev, I. Baruchi, E. Hulata *et al.*, Phys. Rev. Lett. **92**, 118102 (2004).
[13] Y. Ikegaya, G. Aaron, R. Cossart *et al.*, Science **304**, 559 (2004).
[14] M. Bove, S. Martinoia, G. Verreschi *et al.*, Biosens. Bioelectron. **13**, 601 (1998).
[15] Y. Jimbo, A. Kawana, P. Parodi *et al.*, Biol. Cybern. **83**, 1 (2000).
[16] M. W. Oram, M. C. Wiener, R. Lestienne *et al.*, J. Neurophysiol. **81**, 3021 (1999).
[17] B. Derrida and Y. Pomeau, Europhys. Lett. **1**, 45 (1986).
[18] B. Derrida and G. Weisbuch, J. Phys. (France) **47**, 1297 (1986).
[19] A. Wolf, J. B. Swift, H. L. Swinney *et al.*, Physica D (Amsterdam) **16**, 285 (1985).
[20] I. Tsuda, Neural Networks **5**, 313 (1992).
[21] M. N. Shadlen and W. T. Newsome, J. Neurosci. **18**, 3870 (1998).
[22] I. Timofeev, F. Grenier, M. Bazhenov *et al.*, Cereb. Cortex **10**, 1185 (2000).
[23] I. R. Tsang and I. J. Tsang, Phys. Rev. E **60**, 2684 (1999).
[24] W. Maass, T. Natschlager, and H. Markram, Neural Comput. **14**, 2531 (2002).
[25] R. Shaw, Z. Naturfursch, a **36**, 80 (1981).
[26] N. Bertschinger and T. Natschlager, Neural Comput. **16**, 1413 (2004).